

Anomalous Conductance Response of DNA Wires under Stretching

Bo Song,[†] Marcus Elstner,[‡] and Gianaurelio Cuniberti^{*,†}

Institute for Materials Science and Max Bergmann Center of Biomaterials, Dresden University of Technology, D-01062 Dresden, Germany, and Institute for Physical and Theoretical Chemistry, Technical University at Braunschweig, D-38106 Braunschweig, Germany

Received May 30, 2008

ABSTRACT

The complex mechanisms governing charge migration in DNA oligomers reflect the rich structural and electronic properties of the molecule of life. Controlling the mechanical stability of DNA nanowires in charge transport experiments is a requisite for identifying intrinsic issues responsible for long-range charge transfers. By merging density-functional theory based calculations and model Hamiltonian approaches, we have studied DNA quantum transport during the stretching–twisting process of poly(GC) DNA oligomers. During the stretching process, local maxima in the charge transfer integral t between two nearest-neighbor GC pairs arise from the competition between stretching and twisting. This is reflected in local maxima for the conductance, which depend very sensitively on the coupling to the electrodes. In the case of DNA–electrode couplings smaller than t , the conductance versus stretching distance saturates to plateau in agreement with recent experimental observations.

The great interest which DNA attracted in molecular electronic experiments is related to the vision of a truly bottom up electronics at the molecular scale.¹ The very controversial results concerning the conduction of DNA oligomers are ascribable to their internal complexity and their sensitivity to the surrounding environment. It is currently well-accepted² that the mechanisms of charge migration in DNA wires cannot be addressed independently of their mechanical properties.

Recently, magnetic AFM experiments of the Bustamante group³ allowed, while independently stretching and twisting single double stranded DNA oligomers, to access many well-controlled structural configurations of DNA wires. When stretching a short DNA molecule by pulling one of its ends with a standard AFM tip and having the other end fixed on a surface, the angle ϕ between consecutive base pairs reduces from its equilibrium value of 36° . Smaller angle ϕ leads to an increased π – π overlap, resulting in larger charge transfer integrals.^{6–8} On the other hand, the combined twist–stretch process leads increased interbase distances d , effectively decreasing the values of the charge transfer integrals, therefore, antagonizing the effect of twist. This may lead to a complex behavior of the electronic properties of DNA during the stretching process. Interestingly, a nonmonotonous behavior of the transport response of stretched DNA has been

in fact reported by Cohen et al.⁴ and switching and intermittency in DNA break junction experiments have been observed by Kang et al.⁵ As one possible explanation, Kang et al. discussed the change in overlap between neighboring bases as a result of a changed DNA configuration during the stretching process, which has been investigated theoretically before,⁹ however, only for a few geometry snapshots.

In this communication, we investigate the conductance change of DNA along the conformation transition for the stretch–twist process in more detail. Our calculations demonstrate that the charge transfer integrals and the tunneling current show such a nonmonotonic dependence for this process, leading to a switching behavior of the electrical response; the resulting intermitting I – d characteristics may explain the recent experimental findings.^{4,5} Our numerical calculations are further supported by a minimal analytical solvable model.

For this study, we parametrize a model Hamiltonian from the density functional theory based tight binding (DFTB) method.^{10,11} For every geometry snapshot along the stretch–twist path, the effective HOMO–HOMO charge-transfer integral, t , between two nearest-neighbor GC pairs and the effective HOMO level, ϵ , within one GC pair are calculated from DFTB. Subsequently, we use model Hamiltonian methods based on these parameters to estimate the nonequilibrium current–voltage characteristics for bias voltages of the order of the HOMO–LUMO gap.

* Corresponding author. E-mail: g.cuniberti@tu-dresden.de.

[†] Dresden University of Technology.

[‡] Technical University at Braunschweig.

In order to calculate the parameters t and ε , we have implemented in DFTB the molecular fragment orbitals method.¹² The whole molecule is then partitioned into several fragments (shown in Figure 2), consisting of hydrogen bonded base pairs, thereby neglecting the electronically inactive sugars and phosphate groups. Every fragment molecular orbital (FMO) Ψ , which is localized on the base pair, is calculated within DFTB independently, as a linear combination of atomic orbitals, $\Psi_i = \sum_{\mu} c_{\mu,i} \eta_{\mu}$. Here, μ is the index of atomic orbitals (AOs), and i is used for FMOs. Furthermore, we can transform the Kohn–Sham Hamiltonian from the AO picture to the FMO one as follows:

$$H_{ij}^{\text{KS}} = \sum_{\mu,\nu} c_{\mu,i}^* H_{\mu,\nu}^{\text{KS}} c_{\nu,j} \quad (1)$$

Therefore, by means of the method presented in refs 6 and 12, in the case of small overlaps S_{ij} between consecutive FMOs, the HOMO–HOMO charge-transfer integral t between the nearest-neighbor GC pairs can be perturbatively obtained as

$$t_{ij} = H_{ij}^{\text{KS}} - \frac{1}{2}(S_{ij}H_{jj}^{\text{KS}} + H_{ii}^{\text{KS}}S_{ij}) \quad (2)$$

Here, i and j are HOMO indexes for the molecular wire made of consecutive GC-FMOs.

The system we considered consists of a poly(GC) wire containing N base pairs, contacted to left and right electrodes (Figure 2). The resulting Hamiltonian can then be read as follows:

$$H = H_{\text{DNA}} + H_{\text{leads}} + H_{\text{lead-DNA}} \quad (3)$$

with

$$H_{\text{DNA}} = \sum_{i=1}^N \varepsilon_i d_i^\dagger d_i + \frac{1}{2} \sum_{i \neq j} t_{ij} (d_i^\dagger d_j + d_j^\dagger d_i)$$

$$H_{\text{leads}} = \sum_{\alpha,k} \varepsilon_{\alpha,k} c_{\alpha,k}^\dagger c_{\alpha,k}$$

$$H_{\text{lead-DNA}} = \sum_{\alpha=L,k} V_{1,k} (d_1^\dagger c_{\alpha,k} + h.c.) + \sum_{\alpha=R,k} V_{N,k} (d_N^\dagger c_{\alpha,k} + h.c.)$$

where H_{DNA} is a one-dimension chain model for DNA. d_i^\dagger and d_i are the electron operators on the FMO i . The parameters t_{ij} can be obtained from eq 2, while ε_i is the HOMO level of the base pair; α is the lead index, and $c_{\alpha,k}$ are lead electron operators; $\varepsilon_{\alpha,k}$ are k space energies in lead α ; and $H_{\text{lead-DNA}}$ describes the electron hopping between DNA and leads.

The retarded/advanced Green function $G^{r/a}$ can be calculated by means of the equation-of-motion technique:

$$G^{r/a}(\omega) = (\omega I - H_{\text{DNA}} - \Sigma^{r/a}(\omega))^{-1} \quad (4)$$

where I is the identity operator, $\Sigma^{r/a}(\omega) = \Sigma_L^{r/a}(\omega) + \Sigma_R^{r/a}(\omega)$, while $\Sigma_{L,i,j}^{r/a}(\omega) = (-i\Gamma_L \delta_{i,j} \delta_{1,j})/2$, and $\Sigma_{R,i,j}^{r/a}(\omega) = (-i\Gamma_R \delta_{N,i} \delta_{N,j})/2$. Γ_α is the level-width function from lead α .

The current can be obtained by the Landauer formula,

$$I = \frac{2e}{h} \int d\omega T(\omega) [f_L(\omega) - f_R(\omega)] \quad (5)$$

$$T(\omega) = \text{Tr} \{ \tilde{\Gamma}_L G^r \tilde{\Gamma}_R G^a \} \quad (6)$$

with $\tilde{\Gamma}_\alpha = i(\Sigma_\alpha^r - \Sigma_\alpha^a)$, $f_\alpha(\omega)$ is the Fermi function of lead α , and $T(\omega)$ is the transmission function.

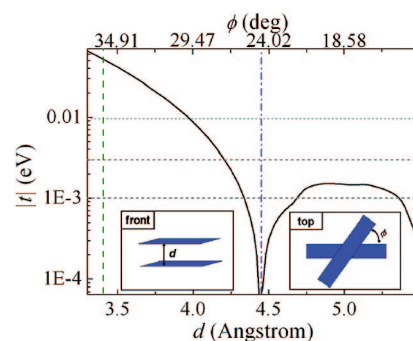


Figure 1. Charge-transfer integral t for the stretching–twisting process as a function of the distance between two GC pairs, d , and the angle ϕ . The green dashed line represents the equilibrium position $d_{\text{eq}} = 3.4 \text{ \AA}$, $\phi_{\text{eq}} = 36^\circ$. The blue dashed-dotted line represents the suppression point ($d_0 \approx 4.45 \text{ \AA}$, $\phi_0 \approx 24.6^\circ$). The three horizontal shot-dashed gray lines are the references used for the intensity of the DNA coupling to the electrodes displayed in Figure 5.

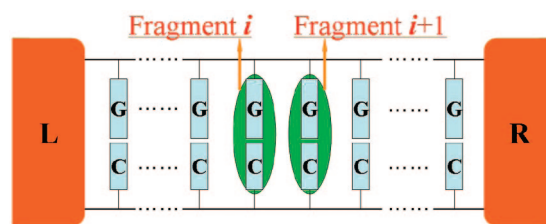


Figure 2. Partition of the DNA molecular junctions for the fragment molecular orbital calculation. See text for details.

The poly(GC) wire stretching–twisting process can be described by in linear response as proposed by the Bustamante group³

$$\Delta\phi = -k\Delta d \quad (7)$$

where $k^{-1} = g/S$, $S = (1100 \pm 200) \text{ pN}$ is the stretch modulus,^{13–16} and $g = 200 \pm 100 \text{ pN}\cdot\text{nm}$ is the stretch–twist coupling.^{15,17–21} The stretching distance is $\Delta d = d - d_{\text{eq}}$, and the twisting angle is $\Delta\phi = \phi - \phi_{\text{eq}}$, while d is the distance between the two nearest-neighbor GC pairs, ϕ is the angle between them, and the subscript “eq” indicates equilibrium position ($d_{\text{eq}} = 3.4 \text{ \AA}$, $\phi_{\text{eq}} = 36^\circ$).

For every molecular mechanic configuration in the stretching–twisting process, the HOMO–HOMO charge-transfer integral t between two GC pairs is then calculated. The results for the transfer integral t are shown in Figure 1: Starting from the equilibrium position, the distance is increased, and the twist angle ϕ is reduced following eq 7; t is first suppressed, and it then exhibits a local maximum. The physics of this process can be understood in terms of the competition between stretching and twisting. As known in the literature,^{6,7} for a pure twisting process (distance $d \equiv d_{\text{eq}}$ is fixed), decreasing the angle ϕ implies a reduction of $|t|$ followed by a rapid increase. For a pure stretching process, $|t|$ is always exponentially suppressed as it happens in tunneling through vacuum. Therefore, the full stretch–twist process can be understood as the dominance of an angle enhanced transfer integral t over pure stretching after the critical value $\phi = \phi_0$ ($d = d_0 \approx 4.45 \text{ \AA}$). Further in the stretching process, the exponentially suppressed distance–

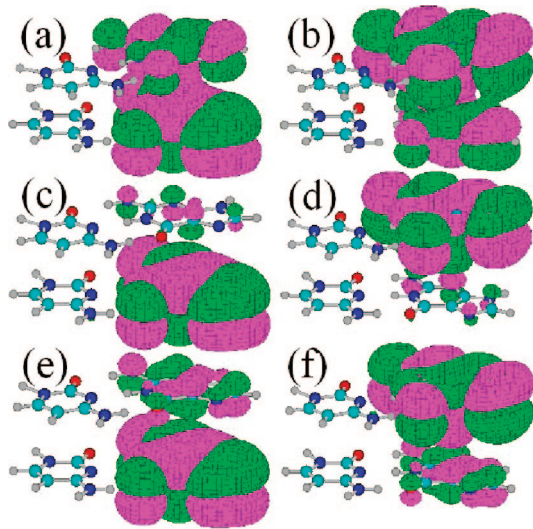


Figure 3. Electron density distribution. (a) HOMO at $d_{\text{eq}} = 3.4 \text{ \AA}$, $\phi_{\text{eq}} = 36^\circ$. (b) HOMO-1 at $d_{\text{eq}} = 3.4 \text{ \AA}$, $\phi_{\text{eq}} = 36^\circ$. (c) HOMO at $d_0 \approx 4.45 \text{ \AA}$, $\phi_0 \approx 24.6^\circ$. (d) HOMO-1 at $d_0 \approx 4.45 \text{ \AA}$, $\phi_0 \approx 24.6^\circ$. (e) HOMO at $d = 5.0 \text{ \AA}$, $\phi = 18.6^\circ$. (f) HOMO-1 at $d = 5.0 \text{ \AA}$, $\phi = 18.6^\circ$.

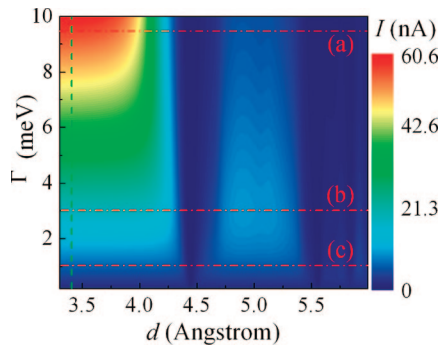


Figure 4. Coupling vs distance dependence of the current I at $V_{\text{bias}} = -2.0 \text{ V}$ for a 30 base pair long poly(GC). Here, $\varepsilon_{\text{GC}} = -1.5 \text{ eV}$, and d is for the distance between two GC pairs. The green dash line is for the equilibrium position ($d_{\text{eq}} = 3.4 \text{ \AA}$).

related tunneling dominates over the increase of the π orbital alignment in the eclipsed configuration.

The physics for this process can also be visualized by means of the density distribution of electrons in the bonding and antibonding orbitals of the two HOMOs (Figure 3). At the equilibrium position, the overlap of the π - π bond from two GC pairs is strong enough (Figure 3a,b). For $\phi = \phi_0$ ($d = d_0$), the HOMO of each GC pair is completely localized (Figure 3c,d). This results in no overlap between the two HOMOs. After that, the HOMO-HOMO overlap is again increased (Figure 3e,f), before being again suppressed because of overdistance tunneling.

Ignoring boundary effect on the level structure of DNA, we can consider site independent quantities $\varepsilon_i \equiv \varepsilon$ and $t_{ij} \equiv t$ in the rest of this work. With these parameters, we investigate the response of the current through a poly(GC) wire in dependence of the different lead-DNA couplings Γ in the stretching-twisting process. We consider here $N = 30$ consecutive base pairs and fix the bias voltage V_{bias} at -2.0 V ; $\varepsilon - E_{\text{F}} = -1.5 \text{ eV}$, where E_{F} is the Fermi level at zero bias.

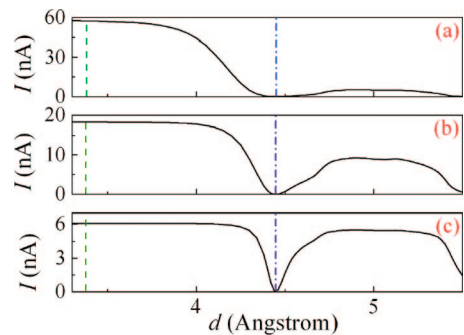


Figure 5. Current–distance relations along the three red (dash-dotted) lines in Figure 4 with same parameters. (a) $\Gamma = 9.5 \text{ meV}$, (b) $\Gamma = 3 \text{ meV}$, (c) $\Gamma = 1 \text{ meV}$. The blue dash-dotted lines are for the position ($d = d_0$, $\phi = \phi_0$).

In DNA nanoelectronic experiments, the backbone is thiol-anchored to gold electrodes, which we model with injection rate values of Γ in the millielectronvolt regime. The calculated current–distance response is shown in Figure 5. Remarkably enough, while reducing the electrode/molecule coupling Γ , the current signal oscillates between equal-height “on” values and suppressed-current “off” values. The presence of such “on” plateau in the stretching–twisting process can be understood by an analytic treatment of the two base pair limit. In this latter case, we can elaborate from eq 6 a formula for the transmission function in dependence of lead-DNA coupling Γ :

$$T(\omega) = \frac{\Gamma^2}{4} \left\{ \frac{1}{(\omega - \varepsilon_+)^2 + (\Gamma/2)^2} + \frac{1}{(\omega - \varepsilon_-)^2 + (\Gamma/2)^2} - \frac{2[(\omega - \varepsilon_+)(\omega - \varepsilon_-) + (\Gamma/2)^2]}{[(\omega - \varepsilon_+)(\omega - \varepsilon_-) + (\Gamma/2)^2]^2 + 4t^2(\Gamma/2)^2} \right\} \quad (8)$$

Here, $\varepsilon_1 = \varepsilon_2 = \varepsilon$, $t_{1,2} = t$, $\Gamma_{\text{L}} = \Gamma_{\text{R}} = \Gamma$, $\Sigma_{\text{L}} = \Sigma_{\text{R}} = -i\Gamma/2$, and $\varepsilon_{\pm} = \varepsilon \pm t$. For the case of $\Gamma \ll t$, at the poles $\omega = \varepsilon_{\pm}$, we can attain the quantum limit $T(\omega) = 1$ independently of t . This explains the emerging of the current “on” plateau.

In conclusion, we have investigated the electrical response of poly(GC) wires under a stretching–twisting mechanical process. In the overstretching regime, we find local maxima for the charge-transfer integral t between two nearest-neighbor GC pairs, arising from the competition between stretching and twisting. This leads to an intermittent current response which strongly depends on the DNA–electrode coupling Γ . For those mechanical configurations, where the transfer integral t is larger than Γ , a current plateau is observed. In the case of experimentally relevant small Γ , several equal height “on/off” switching responses are observed.

These results are supported by the independent experimental observation in the Scheer⁵ and the Porath groups.⁴ Our results suggest that these finding can be understood as a competition of stretching and twisting effects on the charge transfer parameters. The poly(GC) structures presented here serve as a model for the more complex sequences used in experiments. However, the behavior of the t parameters upon stretching and twisting is very similar for other base pair combinations like AG and AA.^{6–8} Therefore, we expect for

other sequences the same qualitative pictures. Of course, dynamic aspects and the effects of solvent are neglected in this model study. During dynamics, the base pairs will fluctuate around equilibrium positions; therefore, proper sampling would have to calculate averages of t and ε along the trajectories. However, it can be expected that the behavior of the averages is qualitatively the same as that for the parameters along the ideal stretching pathway, as considered here. The solvent degrees of freedom lead to fluctuations in the onsite parameters. Again, averages have to be taken, which we assume to be not relevant to understand the qualitative picture.

Acknowledgment. We acknowledge fruitful discussions with Rafael Gutierrez. This work was funded by Deutsche Forschungsgemeinschaft (DFG) within the Project No. CU 44/5-1 of the Priority Program SPP 1243, by the DFG Project No. CU 44/3-2, and by the EU Project No. IST-029192-2 “DNA-based nanoelectronic devices”. Support from the Volkswagen Foundation under Grant I/78 340 is also gratefully acknowledged.

References

- (1) *Lecture Notes in Physics*, Cuniberti G., Fagas G., Richter K., Eds.; Springer: Berlin, 2005; Vol. 68.
- (2) Porath, D.; Cuniberti, G.; Di Felice, R. *Top. Curr. Chem.* **2004**, *237*, 183.
- (3) Gore, J.; Bryant, Z.; Nollmann, M.; Le, M. U.; Cozzarelli, N. R.; Bustamante, C. *Nature* **2006**, *442*, 836.
- (4) Cohen, H.; Nogues, C.; Naaman, R.; Porath, D. *Proc. Natl. Acad. Sci. U.S.A.* **2005**, *102*, 11589.
- (5) Kang, N.; Erbe, A.; Scheer, E. *New J. Phys.* **2008**, *10*, 023030.
- (6) Senthilkumar, K.; Grozema, F. C.; Guerra, C. F.; Bickelhaupt, F. M.; Lewis, F. D.; Berlin, Y. A.; Ratner, M. A.; Siebbeles, L. D. A. *J. Am. Chem. Soc.* **2005**, *127*, 14894.
- (7) Grozema, F. C.; Siebbeles, L. D. A.; Berlin, Y. A.; Ratner, M. A. *ChemPhysChem* **2002**, *3*, 536.
- (8) Felice, R. D.; Calzolari, A.; Molinari, E.; Garbesi, A. *Phys. Rev. B* **2001**, *65*, 045104.
- (9) Maragakis, P.; Barnett, R. L.; Kaxiras, E.; Elstner, M.; Frauenheim, T. *Phys. Rev. B* **2002**, *66*, 241104.
- (10) Elstner, M.; Porezag, D.; Jungnickel, G.; Elsner, J.; Haugk, M.; Frauenheim, T.; Suhai, S.; Seifert, G. *Phys. Rev. B* **1998**, *58*, 7260.
- (11) Frauenheim, T.; Seifert, G.; Elstner, M.; Hajnal, Z.; Jungnickel, G.; Porezag, D.; Suhai, S.; Scholz, R. *Phys. Stat. Sol. B* **2000**, *217*, 41.
- (12) Newton, M. D. *Chem. Rev.* **1991**, *91*, 767.
- (13) Bustamante, C.; Smith, S. B.; Liphardt, J.; Smith, D. *Curr. Opin. Struct. Biol.* **2000**, *10*, 279.
- (14) Bryant, Z.; Stone, M. D.; Gore, J.; Smith, S. B.; Cozzarelli, N. R.; Bustamante, C. *Nature* **2003**, *424*, 338.
- (15) Smith, S. B.; Cui, Y.; Bustamante, C. *Science* **1996**, *271*, 795.
- (16) Wang, M. D.; Yin, H.; Landick, R.; Gelles, J.; Block, S. M. *Biophys. J.* **1997**, *72*, 1335.
- (17) Strick, T. R.; Allemand, J.-F.; Bensimon, D.; Bensimon, A.; Croquette, V. *Science* **1996**, *271*, 1835.
- (18) Marko, J. F. *Europhys. Lett.* **1997**, *38*, 183.
- (19) Kamien, R. D.; Lubensky, T. C.; Nelson, P.; O’Hern, C. S. *Europhys. Lett.* **1997**, *38*, 237.
- (20) Moroz, J. D.; Nelson, P. *Macromolecules* **1998**, *31*, 6333.
- (21) Cluzel, P.; Lebrun, A.; Heller, C.; Lavery, R.; Viovy, J.-L.; Chatenay, D.; Caron, F. *Science* **1996**, *271*, 792.

NL801542G